

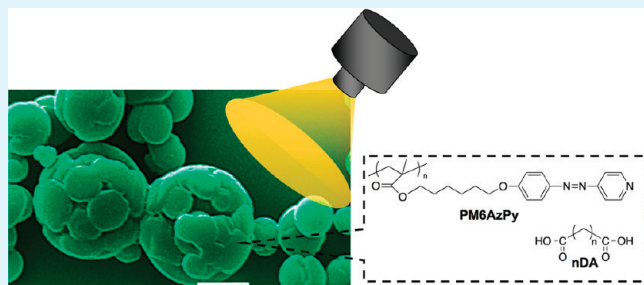
# Fabrication and Photoresponse of Supramolecular Liquid–Crystalline Microparticles

Haifeng Yu,<sup>\*,†,‡</sup> Hui Liu,<sup>‡</sup> and Takaomi Kobayashi<sup>‡</sup>

<sup>†</sup>Top Runner Incubation Center for Academia–Industry Fusion and <sup>‡</sup>Department of Materials Science and Technology, Nagaoka University of Technology, 1603–1 Kamitomioka, 940–2188, Nagaoka, Niigata, Japan

**ABSTRACT:** Supramolecular liquid–crystalline polymer microparticles were fabricated by combining a simple phase reversion method with hydrogen-bonding formation between an azopyridyl polymer and a series of dicarboxylic acid compounds. Their surface morphologies and phase behaviors were studied by changing the molecular length of the diacids, and then their photoresponsive behaviors were observed upon UV irradiation. Photoinduced deformation occurred for the supramolecularly assembled microparticles showing LC phases, whereas no changes in morphologies were observed for microparticles exhibiting amorphous or crystalline. The photoinduced LC-to-isotropic phase transition were responsible for the light-responsive behaviors of the supramolecular liquid–crystalline microparticles.

**KEYWORDS:** supramolecular LC polymers, self–assembly, photofunctionalized microparticles, photoresponsive LC polymers



## INTRODUCTION

Functionalized microparticles is one of the most interesting topics of the present materials science, which significantly enhances their applications in drug–delivery systems,<sup>1</sup> photonics,<sup>2</sup> and electronics.<sup>3</sup> Among them, photoresponsive microparticles have attracted much attention because they provide microscale objects with additional light-responsive functions, like photoinduced change in refractive index, photocontrolled morphologies, and so on.<sup>4–6</sup> Wang et al. fabricated amphiphilic azo polymer colloidal spheres with photoinduced deformation in shape through reprecipitation method.<sup>4,5</sup> Zentel et al. prepared liquid–crystalline (LC) colloidal particles possessing light-switching features through dispersion polymerization.<sup>6</sup> Furthermore, other methods such as emulsion polymerization,<sup>7</sup> seed polymerization,<sup>8</sup> reprecipitation,<sup>9</sup> and microfluidic processes<sup>10</sup> have been employed to prepare such kinds of microparticles. However, these methods have limits, either requiring strictly experimental conditions or containing surfactants remained in the obtained microparticles, which undoubtedly restricts their further applications.

More recently, a phase reversion method called self–organized precipitation (SORP) was employed to prepare polymer microparticles,<sup>11,12</sup> in which microparticles with narrow size distributions were fabricated in mixed solutions of a volatile good solvent and a nonvolatile poor one after evaporation of the good solvent. Although a relative longer time was need for complete evaporation of the volatile solvent and it is difficult for this time-consuming approach to implement in a large scale, this method possessing simple and cost-effective features is suitable for fabricating well-designed microparticles with many kinds of polymers.<sup>11</sup> On the other hand, supramolecular liquid–crystalline polymers (SLCPs) based on hydrogen bonding have been

intensively studied as advanced functional materials.<sup>13,14</sup> If both hydrogen-bond donors and acceptors are involved in the mixed solution using the SORP method, the microparticle precipitation procedure could be accompanied with hydrogen–binding formation since this process simulates the traditional approach for preparation of hydrogen-bonded LC materials by slow evaporation of the solution.<sup>15,16</sup> That means that the formation of polymer microparticles interferes with supramolecular self-assembly, which might supply the fabricated microparticles with some interesting properties, like wrinkled morphologies, LC ordering as well as photoresponsive features, when photosensitive chromophores (e.g., azobenzenes) are involved.<sup>17–23</sup> Especially, the wrinkled surface might provide a large specific surface area for the microparticles, and photoinduced deformation could be more easily observed because of the existence of the free space in the folds. In this paper, we study on fabrication and photoresponsive behaviors of functionalized microparticles composed of SLCPs by combining the phase reversion method with hydrogen–bonded assembling processes.

Generally, carboxylic acids and pyridyl groups have often been used as hydrogen–bond donors and acceptors for preparation of SLCPs with hydrogen bonds as intermolecular interactions.<sup>13–16</sup> Although photoresponsive SLCPs in several condensed states such as powders,<sup>24</sup> films,<sup>25</sup> and fibres<sup>26</sup> have been successfully obtained, to our knowledge, there is no report about fabrication of photofunctionalized SLCP microparticles. Here, we chose an azopyridine–containing polymer PM6AzPy (Figure 1a) as a hydrogen-bond acceptor and a series of

**Received:** January 30, 2011

**Accepted:** March 22, 2011

**Published:** March 22, 2011

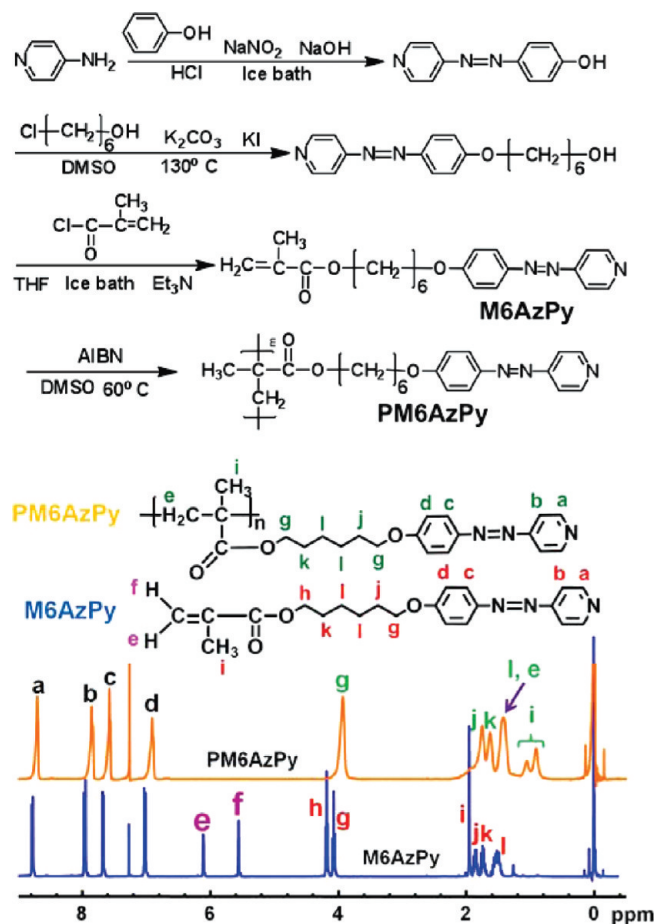


**Figure 1.** Synthetic route (above) and  $^1\text{H}$  NMR spectra (below) of the monomer M6AzPy and the polymer PM6AzPy.

dicarboxylic acids as hydrogen-bond donors for fabricating SLCP microparticles. Confining the photoresponsive azopyridyl moieties with hydrogen-bonded self-assembly in narrow space, multifunctional SLCP microparticles particularly with novel morphologies, and light response are expected.<sup>27</sup>

## EXPERIMENTAL SECTION

The synthetic routes of the azopyridine-containing monomer M6AzPy and the corresponding polymer PM6AzPy are shown in Figure 1.

**Synthesis of 6-(4-(Pyridylazo)phenoxy)hexyl Methacrylate (M6AzPy).** The monomer M6AzPy was synthesized by a diazo-coupling reaction between 4-aminopyridine and phenol in the presence of sodium nitrite and hydrochloric acid and following reactions with 6-chloro-1-hexanol and methacryloyl chloride.<sup>24</sup> The product was purified by silica gel column chromatograph with a mixed solution of ethyl acetate and hexane (1:1, v/v) as eluent, and then an orange powder was obtained with a yield of about 22%. M.p.: 80 °C. UV-vis (chloroform):  $\lambda_{\text{max}} = 356$  nm,  $\epsilon = 5.4 \times 10^3$  L mol<sup>-1</sup> cm<sup>-1</sup>.  $^1\text{H}$  NMR ( $\delta$ , CDCl<sub>3</sub>): 1.43–1.65 (m, 4H), 1.65–1.80 (m, 2H), 1.80–1.90 (m, 2H), 1.96 (s, 3H), 4.08 (t, 2H), 4.19 (t, 2H), 5.56 (s, 1H), 6.12 (s, 1H), 7.03 (d, 2H), 7.69 (d, 2H), 7.96 (d, 2H), 8.79 (d, 2H).

**Synthesis of the Polymer PM6AzPy.** In a 50 mL flask, M6AzPy (1.00, 2.83 mmol) and an initiator azobisisobutyronitrile (AIBN, 4.65 mg, 0.03 mmol) were dissolved in freshly distilled DMF (10 mL). The mixture was deoxygenated by three freeze-pump-thawing cycles and then placed in an oil bath preheated at 60 °C and stirred for 24 h. The polymer

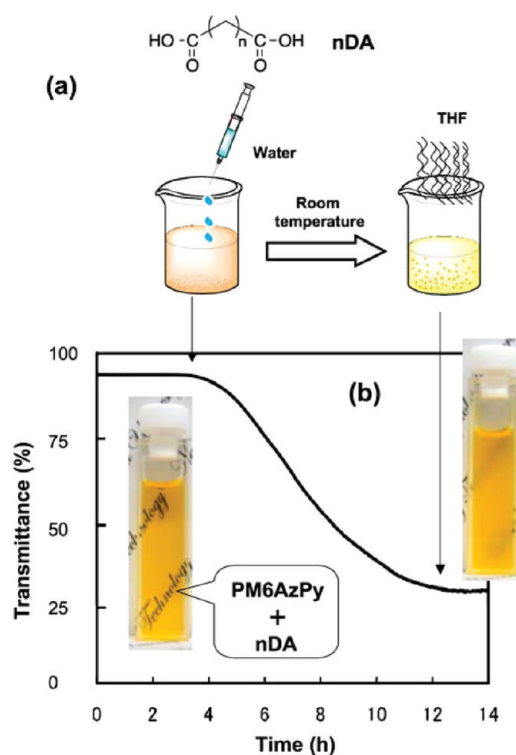


**Figure 2.** (a) Fabrication scheme of the SLCP microparticles and (b) the change in the transmittance measured in situ at 600 nm upon slow evaporation of THF in a mixed solution of PM6AzPy and *n*DA.

was precipitated in hexane and purified with dissolve-precipitate processes with THF and hexane for three times. Then a yellow solid powder was obtained with a yield of 53%. Glass-transition temperature ( $T_g$ ), 42 °C. UV-vis (chloroform):  $\lambda_{\text{max}} = 354$  nm,  $^1\text{H}$  NMR ( $\delta$ , CDCl<sub>3</sub>): 0.79–1.17 (m, 3H), 1.43 (m, 4H), 1.63 (b, 2H), 1.75 (b, 2H), 3.93 (t, 4H), 6.91 (d, 2H), 7.58 (d, 2H), 7.86 (d, 2H), 8.71 (d, 2H).

### Preparation of SLCP (PM6AzPy-*n*DA) Powders and Films.

The SLCP powders were prepared by dissolving PM6AzPy and different dicarboxylic acid compounds (*n*DA,  $n = 1, 4, 6, 9, 10$ ) with equimolar amounts of azopyridyl and acid groups in THF. After slow evaporation of THF at room temperature, the remainder was dried in vacuum for 24 h, and then the SLCP powders were obtained.

The SLCP films were prepared by spin-coating their THF solutions (2.0 wt %) on clean quartz glass substrates at a rotational speed of 1500 rpm. After THF was removed at room temperature, the films were heated to their isotropic states and annealed for 24 h.

**Fabrication of SLCP Microparticles (P-*n*DA).** As shown in Figure 2a, to prepare SLCP microparticles (P-*n*DA), distilled water (5.0 mL) was added dropwise into a clear THF solution (10.0 mL) of the SLCP PM6AzPy-*n*DA (2.0 mg/mL) with vigorously stirring, and then the obtained transparent mixture was left at room temperature to slowly evaporate THF, allowing for gradual formation of microparticles. Finally, the water layer of suspensions was removed, and the remaining microparticles were dried in vacuum for 24 h. For comparison, PM6AzPy microparticles (P-0DA) were also prepared by a similar method without addition of the diacids. All the materials and the corresponding P-*n*DA are summarized in Table 1.

**Photoresponsive Behaviors of SLCP Films and Microparticles.** The obtained SLCP microparticles dispersed in water were dropped into clean glass substrates. After being dried for 2 h and then in a vacuum for 10 h at room temperature, a layer of SLCP microparticles formed on glass surfaces. The samples of microparticles or films were

Table 1. Summary of Thermal Properties of the Dicarboxylic Acids and the Fabricated Materials

melting points (°C) of diacid		thermal properties of SLCP		
		materials	microparticles	<sup>a</sup>
		PM6AzPy	P-0DA	T <sub>g</sub> 42
1DA	134	PM6AzPy-1DA	P-1DA	C 84 I
4DA	153	PM6AzPy-4DA	P-4DA	T <sub>g</sub> 55 LC 95 I
6DA	143	PM6AzPy-6DA	P-6DA	T <sub>g</sub> 54 102 I
9DA	111	PM6AzPy-9DA	P-9DA	T <sub>g</sub> 56 100 I
10DA	129	PM6AzPy-10DA	P-10DA	T <sub>g</sub> 62 109 I

<sup>a</sup> C: crystal; I: isotropic; T<sub>g</sub>: glass transition; LC: liquid crystal.

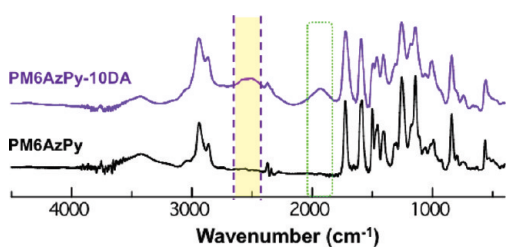


Figure 3. FTIR spectra of PM6AzPy and one SLCP (PM6AzPy-10DA).

irradiated with an unpolarized light beam at 360 nm from a USHIO UV xenon lamp (about 60 mW/cm<sup>2</sup>), putting color filters between the light source and the samples. To observe a large photoinduced deformation, the SLCP microparticles were heated up to a temperature above their T<sub>g</sub> (about T<sub>g</sub> + 10 °C).

**Characterization.** <sup>1</sup>H NMR spectra were recorded on nuclear magnetic resonance spectroscopy (NMR, a JEOL AL-400, 400 MHz for proton) in CDCl<sub>3</sub> solution with tetramethylsilane as an internal reference. FT-IR spectra were determined on a Fourier-transform infrared spectroscope (FT-IR, Shimadzu IR Prestige-21) by putting samples between two NaCl crystals. UV-vis absorption spectra were recorded by using a JUSCO V-630 spectrophotometer. Surface morphologies of the microparticles were investigated with optical microscopy and scanning electronic microscopy (SEM, JSM-5300LV, JEOL). To evaluate LC properties, we used a differential scanning calorimeter (DSC, Thermo plus EVO DSC 8230) and a polarizing optical microscope (POM, ECLIPSE LV100POL, Nikon) with a digital camera (Nikon, DS000).

## RESULTS AND DISCUSSION

As shown in Figure 1, the chemical shifts corresponding to protons in the monomer M6AzPy and the polymer PM6AzPy were accurately assigned in their <sup>1</sup>H NMR spectra, indicating their well-defined molecular structures. Because of the existence of pyridyl groups in azopyridine moieties, such kinds of materials have been intensively studied as hydrogen-bond acceptors for assembling SLCP materials or as ligands for coordination with metal complexes to prepare organic-inorganic hybrid materials.<sup>24-26</sup> Here, azopyridine moieties in PM6AzPy were used as hydrogen-bond acceptors for fabricating SLCPs. Figure 3 shows FT-IR spectra of PM6AzPy and one fabricated SLCP. Being one of powerful tools for characterizing hydrogen-bonding formation,<sup>13-16</sup> FT-IR spectra are often utilized to confirm the structures of the SLCP materials. Comparing the two spectra of PM6AzPy and the SLCP, two additional peaks were clearly observed in that of the SLCP, one peak at 1925 cm<sup>-1</sup> was assigned to Fermi resonance bands, and the other exhibited a

wide peak at around 2545 cm<sup>-1</sup> corresponding to vibration of hydroxyl groups.<sup>26</sup> Other SLCPs also showed similar results in their FTIR spectra. Besides the change in spectra, another effect due to hydrogen-bond formation was that the obtained SLCPs showed better solubility in organic solvents than PM6AzPy and the used diacid compounds.

PM6AzPy was amorphous because of the absence of end substituents in azopyridyl groups, and only a T<sub>g</sub> of about 42 °C was obtained in its DSC curve. Because of the hydrogen-bonding formation, the obtained supramolecular materials showed different thermal properties, which are summarized in Table 1. Upon supramolecular assembly, several changes obviously occurred in the obtained materials. First, the T<sub>g</sub> values of the obtained supramolecular materials were 10 °C higher than that of PM6AzPy because of hydrogen-bonding formation. Second, an additional strong peak was observed in their DSC curves on heating, ascribing to a melting point (PM6AzPy-1DA) or a clearing point (the LC-to-isotropic phase transition) for the SLCPs. Third, their phase transition temperatures were lower than the melting points of the corresponding dicarboxylic acid compounds because the dimers generally existed in the materials containing carboxylic acids were broken by importing azopyridyl groups.<sup>28,29</sup> Furthermore, a strong birefringence was observed in their POM pictures at LC phases, as shown in Figure 4. Undoubtedly, the LC performances benefited from the introduction of nDA with a soft alkyl chain upon supramolecular self-assembly.<sup>13-16</sup>

Then SLCPs microparticles were fabricated with a phase reversion method,<sup>11,12</sup> and the formation processes of microparticles were monitored in situ by measuring the change in the transmittance at 600 nm of the mixed solution.<sup>11</sup> Because of the strong scattering effect of the formed microparticles upon evaporation of THF, the transparent orange solution became turbid (Figure 2b). Surface morphologies of the obtained microparticles were measured with POM and SEM, as shown in Figure 5. Spherical microparticles of P-0DA were clearly observed in Figure 5a, which was further confirmed by their SEM image in Figure 5b. Since the thermodynamic tendency of minimizing the interfacial free energy between different phases usually leads to spherical particles,<sup>12</sup> P-0DA showed a spherical shape with a finely smooth surface, which is similar to other polymer microparticles prepared with the SORP method.<sup>11,12</sup> Moreover, a weak birefringence was observed in the POM picture (Figure 5a), which might arise from the geometrically spherical shape of the amorphous microparticles P-0DA (with a diameter of about 2-3 μm).

In contrast, a strong birefringent image was obtained in Figure 5c upon POM observation. The optical changes must be resulted from the additional LC nature by introducing 10DA



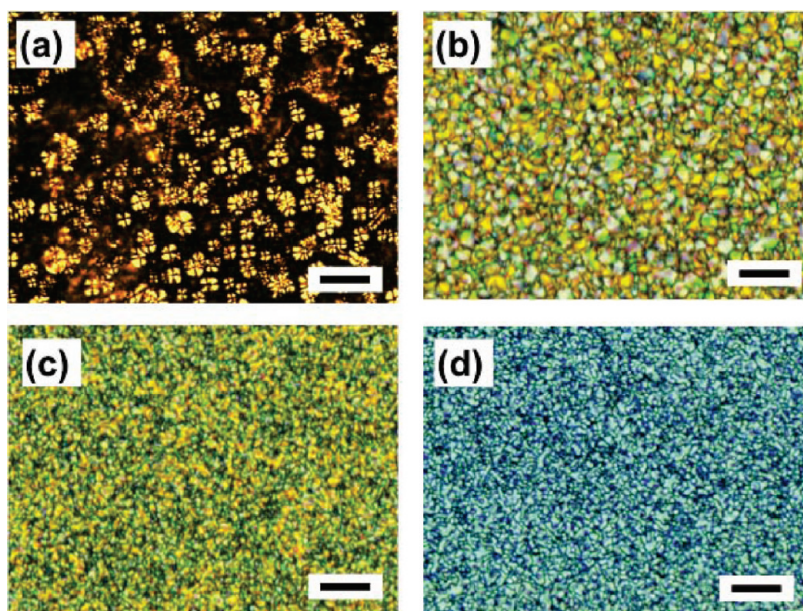


**Figure 4.** POM micrographs of SLCPs: (a) PM6AzPy-4DA at 88 °C, (b) PM6AzPy-6DA at 94 °C, (c) PM6AzPy-9DA at 94 °C, (d) PM6AzPy-10DA at 98 °C. Scale bar is 10  $\mu\text{m}$ .

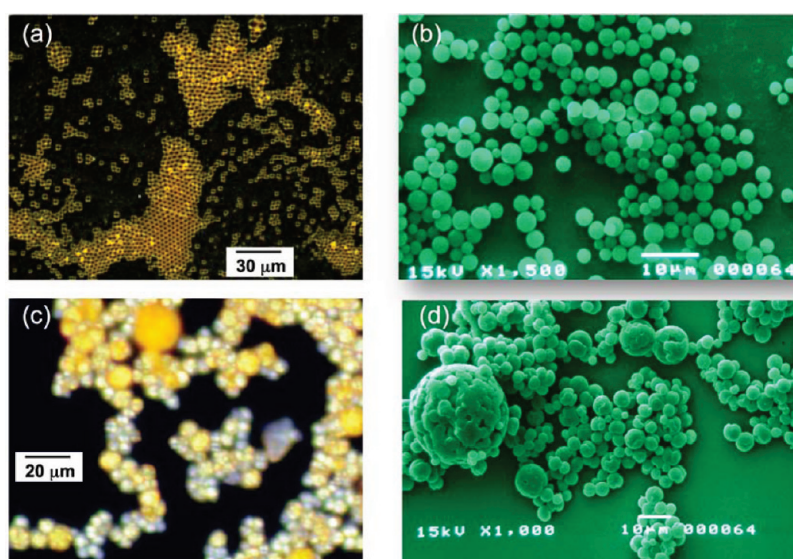


**Figure 5.** Characterization of the fabricated microparticles. (a, b) POM and SEM images of P-0DA, (c, d) POM and SEM images of P-10DA.

into the SLCP. More interestingly, P-10DA exhibited wrinkled morphologies on surface in its SEM image (Figure 5d). The microparticles showed a larger diameter of about 5–12  $\mu\text{m}$ , dispersed among smooth microparticles with a smaller diameter of 1–4  $\mu\text{m}$ . Here, the imported diacid of 10DA could not only serve as end groups to form mesogenic groups by hydrogen bonding with azopyridyl moieties, but also function as weak cross-linkages because both ends of 10DA are carboxylic acids showing hydrogen-bond donor capability, leading to the formation of these fascinating wrinkled SLCP microparticles.

To understand the LC effect on the wrinkled morphologies, other SLCP microparticles P-1DA, P-4DA, P-6DA, and P-9DA were also studied, and their SEM images with a larger

magnification are given in Figure 6. Among them, P-1DA showed a crystalline phase, whereas P-4DA, P-6DA, and P-9DA exhibited ordered LC phases. With a similar size (a diameter in 2–5  $\mu\text{m}$ ), P-1DA, P-4DA, and P-6DA also demonstrated smooth surfaces, but wrinkled morphologies were observed in P-9DA. These indicated that LC ordering of the SLCPs was not one of the necessary factors for fabricating microparticles with wrinkled morphologies. Considering molecular structures of the diacids, 9DA and 10DA with relative longer structures of soft alkylene chains could provide the fabricated SLCPs with free volumes, larger enough for aggregations and assembly in the fabrication processes of phase reversion, bringing about the SLCP microparticles with wrinkled surfaces. Besides, such wrinkled surfaces were also observed in

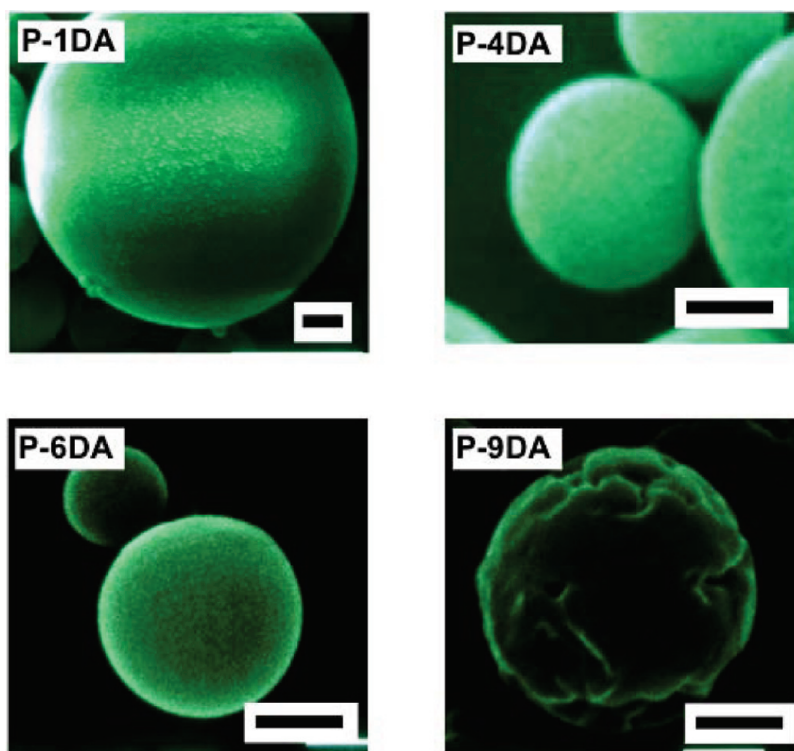


**Figure 6.** SEM pictures of supramolecular microparticles P-*n*DA with a larger magnification. The scale bar represents 1  $\mu\text{m}$ .

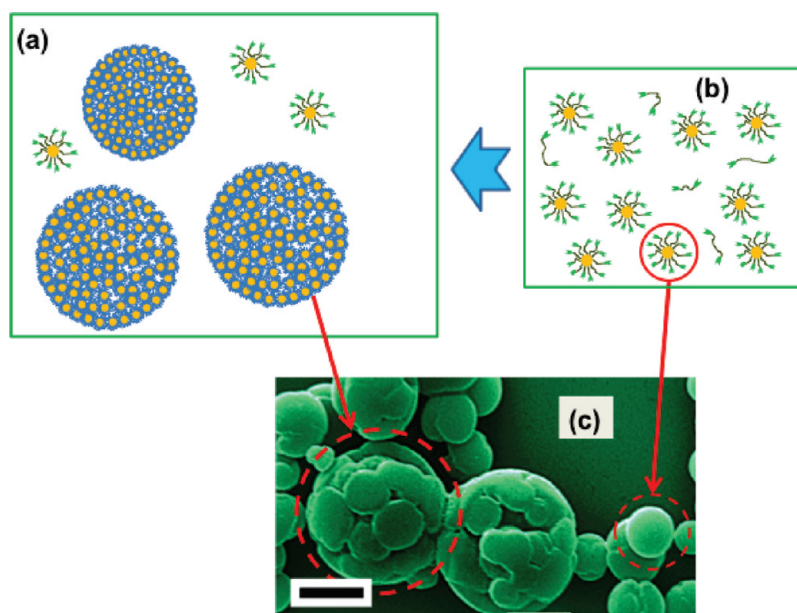


**Figure 7.** Possible illustration of formation of the SLCP microparticles with wrinkled morphologies in the second stage.

poly(methyl methacrylate) microparticles prepared by dispersed polymerization when the concentration of the cross-linker (divinylbenzene) was higher than 6 wt %.<sup>30</sup> It was reported that cross-linkers at the nucleation stage played an important role in preparation of such microparticles with deformed morphologies.<sup>31</sup> In the present system, the diacid acting as cross-linkers had a high concentration (50 mol %). Although the formation mechanism of wrinkled microparticles was unclear, the diacid should

play a similar role in the nucleation stage for fabricating the SLCP microparticles to that in dispersion polymerization.<sup>30,31</sup>

A possible scheme is proposed in Figure 7 to describe surface morphology transformation of the fabricated SLCP microparticles, in which two stages might be included in the SLCP microparticle formation. The first stage is similar to the SORP process reported by Shimomura et al.,<sup>11,12</sup> and microparticles with smooth surfaces were obtained. At this stage, the formed small



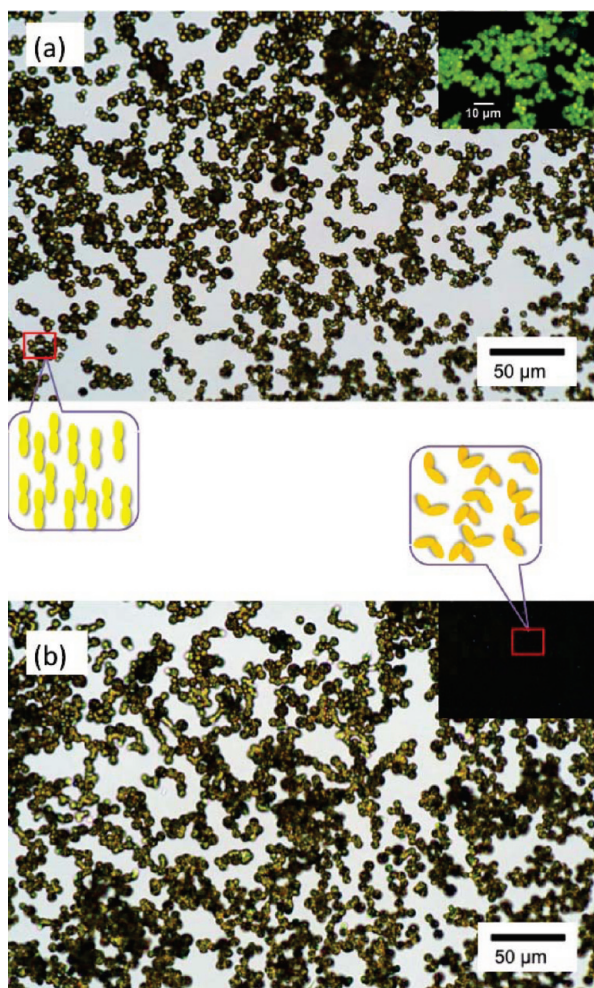


**Figure 8.** Microscopic pictures of P-10DA (a) before and (b) after UV irradiation at 360 nm (at 75 °C). Both photoinduced phase transition and deformation of the SLCP microparticles occurred. Onset pictures are POM images.

particles showed LC properties due to supramolecular self-assembly, probably with free carboxylic acid groups on the surface. That means that a fairly strong surface tension existed at the surface of the small particles. Then aggregation of such small particles occurred because of the weak cross-linking induced by the diacid, leading to formation of the “superspheres” with wrinkled surfaces. The longer of the alkylene in the *n*DA, the better of the second stage could proceed. It must be mentioned that the agglomerated particles still seemed to have spherical surfaces, albeit having occasional gaps. This is because not all of the small particles aggregated together since two carboxylic groups in *n*DA might be occupied by one microparticle. For this case, the obtained microparticles showed a smaller size and smooth surface. Obviously, the second stage might be responsible for the formation of the wrinkled morphologies. The diacid with a shorter alkylene (1DA, 4DA, 6DA) did not cause efficient agglomeration in the second state, resulting in smooth microparticles as prepared using the SORP method without addition of the diacid. Considering the high possibility of two carboxylic groups in *n*DA with a shorter alkylene being occupied by one particle, not all of the small particles aggregated together, leading to the heterogeneity in sample size upon preparation of the SLCP microparticles.

Apart from the hydrogen-bonding formation property, photoresponse is another interesting performance of the azopyridyl moieties in the SLCPs because of the existence of light-sensitive groups. Generally, an azobenzene group can act as both a chromophore and a mesogens,<sup>27</sup> and photoinduced phase transition has been induced upon UV irradiation because *trans*-azobenzene might be LC and its *cis*-isomer never shows mesogenic phases.<sup>27,32</sup> Here, the azopyridyl group in the SLCP microparticles might play the same role even though the LC ordering obtained from the supramolecular hydrogen-bonds are confined in the narrow space of microparticles.<sup>33</sup> Then photoresponse of the fabricated SLCPs were studied with UV irradiation. As shown in Figure 8, deformation of the SLCP microparticles (P-10DA) was clearly observed upon UV irradiation at 360 nm. In this photo irradiation process, it seems that the SLCP microparticles were first softened and then broken like a water drop because of the function of gravitational force. Several adjacent microparticles in the softening state merged into irregular objects shown in Figure 8b.

In situ heating P-10DA samples on glass substrates were carried out to measure their thermal stability with POM observation. They were not broken until being heated up a temperature higher its clear point (109 °C). To get rid of thermal effect in light irradiation, heat-absorption glass filters were used in the optical setup. Within a irradiation time of 30 min, the temperature of the samples was increased by about 2 °C, which demonstrated that the distortion of P-10DA was not induced by thermal effect, but the actinic light. Furthermore, the birefringence of the SLCPs almost disappeared after the photo irradiation accompanying with the light-induced deformation, as indicated by the POM pictures in the onset of Figure 8. These demonstrated that LC-to-isotropic phase transition was photoinduced in the SLCPs, which might be responsible for the deformation. Upon irradiation of linearly polarized UV light, similar photoresponsive results were also observed in the SLCP microparticles, which is different from the anisotropic deformation of amorphous colloidal spheres reported by Wang et al.<sup>4,5</sup> These showed that the light responsive behaviors of the SLCP microparticles were insensitive to the polarization of the actinic light. Recently, Zentel et al. prepared LC microparticles with covalently cross-linked structures.<sup>6,10,34</sup> Photoinduced phase transition or change in LC alignment occurred for the obtained microparticles upon UV irradiation, leading to their shape deformation from sphere to ellipsoid. But no bursting was observed because of the existence of strong cross-linking function by covalent bonds.<sup>34</sup> In P-10DA, the weak cross-linking due to hydrogen bonding could not greatly improve the mechanical properties of the microparticles, resulting in photoinduced deformation in Figure 8.

Other SLCP microparticles (P-9DA, P-6DA, and P-4DA) exhibited analogous photoresponsive behaviors to that of P-10DA. Far differently, both amorphous P-0DA and crystalline P-1DA microparticles were not deformed with light irradiation, although photoisomerization of azopyridyl groups was obviously induced. This also confirmed that the photoinduced deformation of the SLCP microparticles might be resulted from the photoinduced phase transition of the SLCPs, which is seldom observed in amorphous or crystallized materials.<sup>35</sup>

To explicitly illustrate the photoresponsive behaviors of the SLCP microparticles, we studied the absorption spectra of SLCPs in films. As shown in Figure 9a,c, the maximum absorption peak in UV-vis absorption spectra for both PM6AzPy and its SLCP (PM6AzPy-10DA) was at around 351 nm, because of

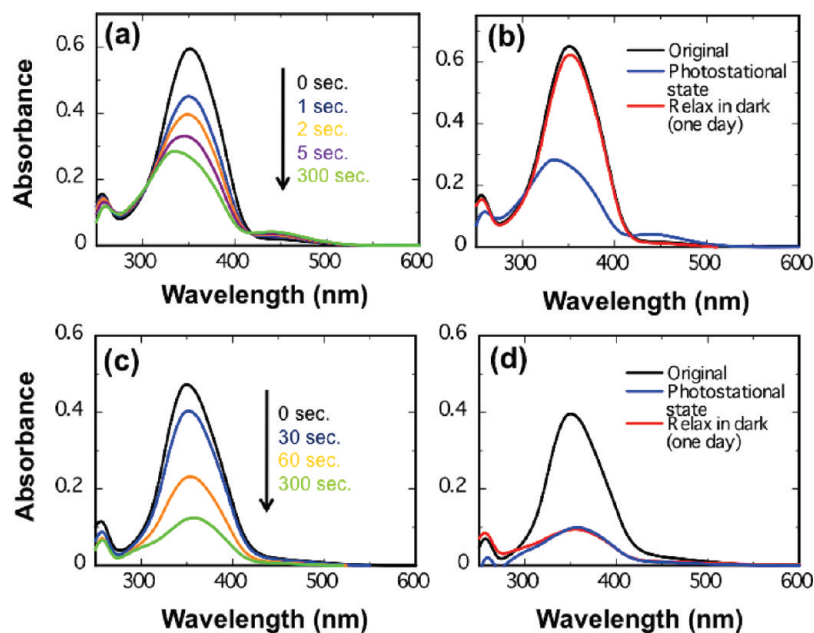


**Figure 9.** UV–vis absorption spectra of thin polymer films. (a) PM6AzPy upon irradiation of UV light, (b) PM6AzPy relaxed in dark, (c) PM6AzPy–10DA upon irradiation of UV light, (d) PM6AzPy–10DA relaxed in dark.

the  $\pi$ – $\pi^*$  transition of azopyridyl groups.<sup>36,37</sup> This peak decreased upon UV irradiation, whereas another absorption peak at about 450 nm due to the  $n$ – $\pi^*$  transition of azopyridyl groups gradually increased, as a result of *trans*–*cis* photoisomerization. Although the change tendency of Figure 9a,c was similar, the SLCP exhibited a slower photoresponsive speed than PM6AzPy. Because the end of the azopyridyl moiety was restricted by an acid group via hydrogen bonding in the SLCP, its activity for change in molecular configuration was lower than that of non-bonded conditions in PM6AzPy, resulting in a delaying photoresponse.<sup>24</sup> In the photostationary state, the SLCP showed a higher isomerization degree than that of PM6AzPy. Being stored in dark, the spectrum of PM6AzPy almost relaxed to its original state because of back *cis*–*trans* isomerization (Figure 9b). In contrast, no obvious changes occurred in the spectrum of the SLCP after one day's relaxation (Figure 9d), indicating the stable phase state of the *cis* isomer in the SLCP film.

The different photoresponse of PM6AzPy and its SLCPs might originate from their dissimilar condensed phase structures. The former was amorphous and the latter showed supramolecularly assembled LC phases. Isomerization of azopyridine groups in PM6AzPy only caused little change in material properties since no phase transition occurred. Things are different for its SLCPs, and an LC-to-isotropic phase transition was induced by the isomerization of azopyridine groups, as shown in Figure 10. This photochemical reaction of the SLCPs resulted in almost disappearance of optical birefringence in its POM pictures. Because of the stable *cis* isomers of azopyridyl groups in the SLCPs (Figure 9d), the photoinduced isotropic state in films showed good stability under room light, and no obvious changes were measured with POM observation and UV–vis absorption spectra after being stored for one week.

Therefore, the photoinduced deformation of the SLCP microparticles was attributed to the LC-to-isotropic phase transition upon UV irradiation. The conformation changes of the azopyridine groups in the SLCP microparticles can be described

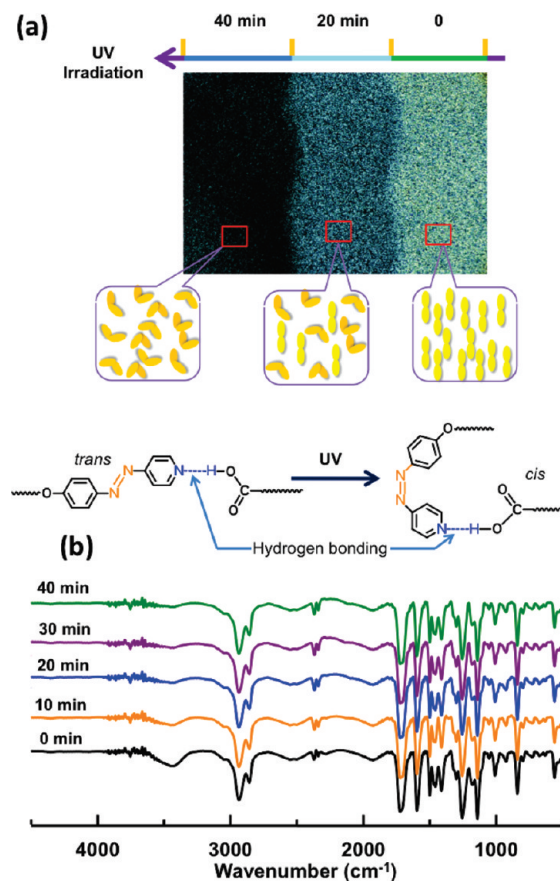


**Figure 10.** Photoresponse of the PM6AzPy–10DA film. (a) POM image and (b) FTIR spectra.

in Figure 8. In the photochemical reactions of SLCPs, the hydrogen bonds between azopyridine and carboxylic groups



exhibited a higher stability, similar to that of covalent bonds. Their characteristic peaks at 1925 and 2545  $\text{cm}^{-1}$  in FT-IR spectra remained unchangeable even being photoinduced into an isotropic phase in Figure 10b. Analogously to azobenzene-containing LC materials, visible light can induce back isotropic-to-LC phase transition, but the deformed SLCP microparticles were not restored because the weak cross-linked functions induced by hydrogen bonding are not strong enough as that in elastomers cross-linked with covalent bonds.<sup>38–41</sup>

## CONCLUSION

In summary, photoresponsive SLCP microparticles were successfully fabricated by combining a simple phase reversion method with hydrogen-bonding formation between PM6AzPy and a series of dicarboxylic acids. The formation of polymer microparticles interfered with supramolecular self-assembly provided the fabricated SLCP microparticles with wrinkled morphologies, LC ordering as well as photoresponsive features. The length of diacids *n*DA played an important role in the formation of the SLCP microparticles with wrinkled morphologies upon self-assembly, and smooth spherical SLCP microparticles were obtained with a shorter diacid or without addition of the diacid. Because of the existence of photoisomerizable azopyridyl groups and LC ordering in SLCPs, photoinduced phase transition was observed upon UV irradiation, resulting in deformed shape in the SLCP microparticles. The hydrogen bonds showed good stability upon photo irradiation. The fabricated SLCP microparticles possessed both light-responsive LC nature and fascinating morphologies, which makes them promising for advanced applications in photonics and actuators.

## AUTHOR INFORMATION

### Corresponding Author

\*E-mail: yuhaifeng@mst.nagaokaut.ac.jp. Tel: +81-0258-47-8416. Fax: +81-0258-47-9300.

## REFERENCES

- (1) Otsuka, H.; Nagasaki, Y.; Kataoka, K. *Adv. Drug Delivery Rev.* **2003**, *55*, 403.
- (2) Yin, Y.; Xia, Y. *Adv. Mater.* **2002**, *14*, 605.
- (3) Wang, X.; Summers, C.; Wang, Z. *Nano Lett.* **2004**, *4*, 423.
- (4) Li, Y.; He, Y.; Tong, X.; Wang, X. *J. Am. Chem. Soc.* **2005**, *127*, 2402.
- (5) Li, Y.; Tong, X.; He, Y.; Wang, X. *J. Am. Chem. Soc.* **2006**, *128*, 2220.
- (6) Vennes, M.; Zentel, R. *Macromol. Chem. Phys.* **2004**, *205*, 2303.
- (7) Chevalier, Y. *Curr. Opin. Colloid Interface Sci.* **2002**, *7*, 3.
- (8) Karlsson, O.; Hassander, H.; Wesslén, B. *J. Appl. Polym. Sci.* **1997**, *63*, 1543.
- (9) Kasai, H.; Nalwa, H.; Oikawa, H.; Okada, S.; Matsuda, H.; Minami, N.; Kakuta, A.; Ono, K.; Mukoh, A.; Nakanishi, H. *Jpn. J. Appl. Phys.* **1992**, *31*, 1132.
- (10) Ohm, C.; Fleischmann, E.; Kraus, I.; Serra, C.; Zentel, R. *Adv. Funct. Mater.* **2010**, *20*, 4314.
- (11) Yabu, H.; Higuchi, T.; Ijio, K.; Shimomura, M. *Chaos* **2005**, *15*, 047505.
- (12) Yabu, H.; Tajima, A.; Higuchi, T.; Shimomura, M. *Chem. Commun.* **2008**, 4588.
- (13) Kato, T.; Mizoshita, N.; Kishimoto, K. *Angew. Chem., Int. Ed.* **2006**, *45*, 38.
- (14) Kato, T.; Fréchet, M. J. *Liq. Cryst.* **2006**, *33*, 1429.
- (15) Kato, T.; Fréchet, J. J. *Am. Chem. Soc.* **1989**, *111*, 8533.

- (16) Kumar, U.; Kato, T.; Fréchet, J. J. *Am. Chem. Soc.* **1992**, *114*, 6630.
- (17) Yu, H. F.; Naka, Y.; Shishido, A.; Ikeda, T. *Macromolecules* **2008**, *41*, 7959.
- (18) Yu, H. F.; Ikeda, T.; Iyoda, T. *J. Am. Chem. Soc.* **2006**, *128*, 11010.
- (19) Han, D.; Tong, X.; Zhao, Y.; Zhao, Y. *Angew. Chem., Int. Ed.* **2010**, *49*, 9162.
- (20) Zhao, Y.; He, J. *Soft Matter* **2009**, *5*, 2686.
- (21) Shishido, A. *Polym. J.* **2010**, *42*, 525.
- (22) Seki, T.; Nagano, S. *Chem. Lett.* **2008**, *37*, 484.
- (23) Kausar, A.; Nagano, H.; Ogata, T.; Nonaka, T.; Kurihara, S. *Angew. Chem., Int. Ed.* **2009**, *48*, 2144.
- (24) Cui, L.; Zhao, Y. *Chem. Mater.* **2004**, *16*, 2076.
- (25) Mamiya, J.; Yoshitake, A.; Kondo, M.; Yu, Y.; Ikeda, T. *J. Mater. Chem.* **2008**, *18*, 63.
- (26) Aoki, K.; Nakagawa, M.; Ichimura, K. *J. Am. Chem. Soc.* **2000**, *122*, 10997.
- (27) Yu, H. F.; Ikeda, T. *Adv. Mater.* **2011** in press.
- (28) Johnson, S. L.; Rumon, K. A. *J. Phys. Chem.* **1965**, *69*, 74.
- (29) Schrier, E.; Pottle, M.; Scheraga, H. *J. Am. Chem. Soc.* **1964**, *86*, 3444.
- (30) Lee, K. C.; Lee, S. Y. *Macromol. Res.* **2007**, *15*, 244.
- (31) Lee, K. C.; Lee, S. Y. *Macromol. Res.* **2008**, *16*, 294.
- (32) Yu, H. F.; Kobayashi, T. *Molecules* **2010**, *15*, 570.
- (33) Yu, H. F.; Asaoka, S.; Shishido, A.; Iyoda, T.; Ikeda, T. *Small* **2007**, *3*, 768.
- (34) Ohm, C.; Serra, C.; Zentel, R. *Adv. Mater.* **2009**, *21*, 4859.
- (35) Ichimura, K. *Chem. Commun.* **2009**, 1496.
- (36) Yu, H. F.; Iyoda, T.; Okano, K.; Shishido, A.; Ikeda, T. *Mol. Cryst. Liq. Cryst.* **2005**, *443*, 191.
- (37) Yager, K. G.; Barrett, C. J. *J. Photochem. Photobiol. A: Chem.* **2006**, *182*, 250.
- (38) Barrett, C. J.; Yager, K. G.; Mamiya, J.; Ikeda, T. *Soft Matter* **2007**, *2*, 1249.
- (39) He, J.; Zhao, Y.; Zhao, Y. *Soft Matter* **2009**, *5*, 308.
- (40) Camacho-Lopez, M.; Finkelmann, H.; Palffy-Muhoray, P.; Shelley, M. *Nat. Mater.* **2004**, *3*, 307.
- (41) Yang, H.; Buguin, A.; Taulemesse, J. M.; Kaneko, K.; Méry, S.; Bergeret, A.; Keller, P. *J. Am. Chem. Soc.* **2009**, *131*, 15000.